

Thermoelectric response as a tool to observe electrocaloric effect in a thin conducting ferroelectric SnSe flake

N.N. Orlova,¹ A.V. Timonina,¹ N.N. Kolesnikov,¹ and E.V. Deviatov¹

¹*Institute of Solid State Physics of the Russian Academy of Sciences,
Chernogolovka, Moscow District, 2 Academician Ossipyan str., 142432 Russia*

(Dated: July 14, 2021)

We experimentally investigate thermoelectric response of a 100 nm thick SnSe single crystal flake under the current-induced dc electric field. Thermoelectric response appears as a second-harmonic transverse voltage $V_{xy}^{2\omega}$, which reflects temperature gradient across the sample due to the Joule heating by harmonic ac excitation current I_{ac} . In addition to strongly non-monotonous dependence $V_{xy}^{2\omega}$, we observe that dc field direction controls the sign of the temperature gradient in the SnSe flake. We provide arguments, that electrocaloric effect is the mostly probable reason for the results obtained. Thus, our experiment can be understood as demonstration of the possibility to induce electrocaloric effect by in-plane electric field in conducting ferroelectric crystals and to detect it by thermoelectric response.

PACS numbers: 71.30.+h, 72.15.Rn, 73.43.Nq

INTRODUCTION

Recent interest to conductors with broken inversion symmetry is connected not only with topological materials [1], but also with conducting ferromagnetic and ferroelectric crystals. For ferromagnetic conductors with spin-orbit coupling, current-induced spin polarization leads to spin-orbit torques [2], which opens a new field in spintronics. In ferroelectrics, current-induced electric field opens a way to control ferroelectric polarization in polar crystals. The latter effect can be expected for mono- or di-chalcogenides of transitional metals like WTe₂, SnS, SnSe, etc. [3, 4], or for monolayer-based artificial structures [5, 6].

One of the sophisticated phenomena in ferromagnetic or ferroelectric systems is the caloric effect, which is also important for applications. For example, it can be useful in development of new refrigeration technologies and materials [7, 8] and cooling/heating environmentally friendly devices [9] or renewable energy sources [10, 11]. Magnetocaloric and electrocaloric effects occur due to the entropy difference between (ferromagnetically or ferroelectrically) ordered or disordered states, which can be controlled by applying or removing of the external magnetic or electric fields, respectively [8, 12]. For the electrocaloric effect, this difference leads to the temperature variation if the ferroelectric polarization changes at stable entropy experimental environments [13, 14]. Recent experimental investigations are performed for insulating ferroelectric crystals [8] or thin films [12, 14, 15], which are placed between two metallic capacitor plates. Electrocaloric effect is controlled by external out-of-plane electric field in this case. In addition to general fundamental problems [11, 13], applied research is mostly intended to improve the caloric effect in lead-free insulating materials [8, 16].

On the other hand, electrocaloric effect should prin-

cipally be observable in ferroelectric conductors. Ferroelectric polarization is also sensitive to current-induced electric field in conducting structures, which is impossible for ferroelectric insulators. Even for small absolute values of the effect, corresponding temperature gradients should be detectable by in-situ thermoelectric response measurements [18–20]. Among different materials, layered SnSe single crystals can be convenient for these investigations: thin SnSe flakes (300 nm and below) are characterized by the in-plane ferroelectric polarization [22, 23] in addition to significant thermoelectric properties [21].

Here, we experimentally investigate thermoelectric response of a 100 nm thick SnSe single crystal flake under the current-induced dc electric field. Thermoelectric response appears as a second-harmonic transverse voltage $V_{xy}^{2\omega}$, which reflects temperature gradient across the sample due to the Joule heating by harmonic ac excitation current I_{ac} . In addition to strongly non-monotonous dependence $V_{xy}^{2\omega}$, we observe that dc field direction controls the sign of the temperature gradient in the SnSe flake. We provide arguments, that electrocaloric effect is the mostly probable reason for the results obtained. Thus, our experiment can be understood as demonstration of the possibility to induce electrocaloric effect by in-plane electric field in conducting ferroelectric crystals and to detect it by thermoelectric response.

SAMPLES AND TECHNIQUES

SnSe compound was synthesized by reaction of selenium vapors with the melt of high-purity tin in evacuated silica ampoules. The SnSe layered single crystal was grown by vertical zone melting in silica crucibles under argon pressure. The structure of single crystal is verified by X-ray diffraction methods. The initial SnSe is characterized the layered structure with orthorhombic crystal

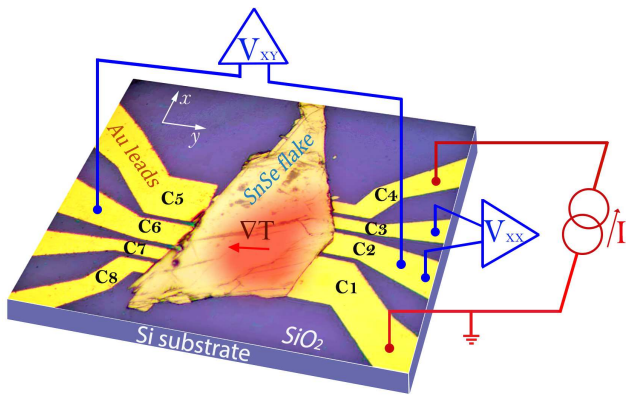


Figure 1. (Color online) Optical image of a typical sample with a sketch of electrical connections. 200 nm thick SnSe flake is placed on the top of the pre-defined Au leads pattern, the 5 μm separated Au leads specifies experimental geometry for thermoelectric and charge transport investigations. For thermoelectric measurements, thermal gradient ∇T is created by ac current $\sim \cos(\omega t)$ between two Au-SnSe contacts C1 and C4 due to the Joule heating of the sample, $\nabla T \sim \cos(2\omega t)$ is perpendicular to the current line. Thus, we detect thermoelectric response as the second-harmonic transverse ac voltage $V_{xy}^{2\omega} \sim \cos(2\omega t)$ between contacts C2 and C6.

system [23].

In layered monochalcogenides, ferroelectricity appears below some critical thickness [3], which can be estimated [24] as 300 nm for SnSe. Ferroelectric polarization is due to the distortion of centrosymmetric $Pnma$ orthorhombic structure at low thicknesses, which appears as polar orthorhombic $P2_1mn$ space group [22]. In particular, anisotropy of the Raman intensity is investigated vs. the SnSe flake thickness in Ref. [24]. The observed anisotropy has been connected with crystal symmetry group. It has been shown, that SnSe symmetry is highest for the bulk material, while unique in-plane anisotropic phonon behavior is observed for the SnSe flake thickness from 300 nm and down to the few-layer samples [24].

Ultra-thin [23] SnSe flakes (about 100-200 nm) are obtained by regular mechanical exfoliation from the initial layered ingot. For electrical measurements the exfoliated flake is placed on the top of the pre-defined Au leads pattern, the pattern specifies experimental geometry for charge transport as it is depicted in Fig. 1. Standard photolithography and lift-off technique are used to define 100 nm thick Au leads on the insulating SiO_2 substrate. This procedure has been verified to provide electrically stable contacts with highly transparent metal-semiconductor interfaces, see Refs. [25, 26], and, simultaneously, it minimizes chemical or thermal treatment of the initial flake [27]. It is also important, that the relevant (bottom) SnSe flake surface is protected from any oxidation or contamination by SiO_2 substrate.

Resistance of the investigated samples varies from 1 kOhm to 20 kOhm, an actual value depends mostly on the overlap area between SnSe flake and Au leads in Fig. 1.

For thermoelectric measurements we use four-point lock-in technique with second harmonic detection [18–20]. Thermal gradient is created by ac current $I_{ac}\cos(\omega t)$ applied between two Au-SnSe heating contacts C1 and C4, see Fig. 1, which we refer as x axis. Thermal gradient appears due to the Joule heating of the sample $\nabla T \sim (I_{ac})^2\cos(2\omega t)$, it is perpendicular to the current line in Fig. 1. For this reason, we detect thermoelectric response as the second-harmonic transverse (i.e. along y axis) voltage $V_{xy}^{2\omega}$ between contacts C2 and C6. To obtain $V_{xy}^{2\omega}$ dependence on the in-plane electric field, we additionally apply high dc current I_{dc} between the same heating contacts in Fig. 1. We wish to note, that longitudinal (along x) dc current can not directly contribute to the transverse (along y) $V_{xy}^{2\omega}$ second-harmonic ac response.

Amplitude and frequency of I_{ac} is verified to have the correct Ohmic behavior of the longitudinal first harmonic $V_{xx}^{1\omega}$ component. In particular, I_{ac} is below 10 μA at the frequency of 1.7 kHz. I_{dc} is swept within ± 1 mA range, which corresponds to 10^9 A/m² current density for our dimensions, and to in-plane electric field 10^5 V/m for 1 kOhm sample resistance. All measurements are performed at room temperature.

EXPERIMENTAL RESULTS

Fig. 2 shows typical examples of four-point longitudinal (along x) $V_{xx}^{1\omega}$, $V_{xx}^{2\omega}$ and transverse $V_{xy}^{1\omega}$, $V_{xy}^{2\omega}$ voltage components in dependence on the ac current amplitude I_{ac} . The first harmonic longitudinal voltage $V_{xx}^{1\omega}$ component demonstrates standard Ohmic behavior $V_{xx}^{1\omega} = RI_{ac}$ with four-point sample resistance $R = 1.2$ kOhm, see Fig. 2 (a). The first harmonic transverse voltage $V_{xy}^{1\omega}$ is much smaller, it seems to appear due to the contacts mismatch. Ohmic behavior is also confirmed by nearly zero second-harmonic longitudinal $V_{xx}^{2\omega}$ component in Fig. 2 (b). In contrast, there is significant transverse second-harmonic voltage $V_{xy}^{2\omega}$ in Fig. 2 (b). $V_{xy}^{2\omega}$ it is clearly non-linear and follows to $(I_{ac})^2$ law, as depicted in the inset to Fig. 2 (b). This behavior well corresponds to thermoelectric origin of $V_{xx}^{2\omega} \sim \nabla T$, where the temperature gradient ∇T is defined by Joule heating of the sample $\nabla T \sim (I_{ac})^2\cos(2\omega t)$. One can estimate maximum temperature difference ΔT as ≈ 0.5 K between contacts C6 and C2 for the known [21] SnSe thermoelectric coefficient $520\mu\text{V/K}$.

Our main result is the dependence of the thermoelectric response $V_{xy}^{2\omega}$ on the dc bias current I_{dc} , which is applied between the same contacts C1 and C4 as the ac current component. The experimental $V_{xy}^{2\omega}(I_{dc})$ curve

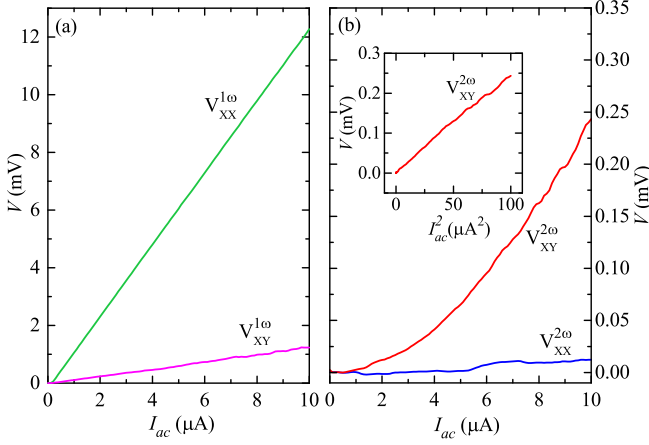


Figure 2. (Color online) (a) The first harmonic longitudinal voltage $V_{xx}^{1\omega}$ component in dependence on the ac current I_{ac} amplitude. It demonstrates standard Ohmic behavior $V_{xx}^{1\omega} \sim I_{ac}$ with corresponding four-point sample resistance value $R = 1.2$ kOhm. The first harmonic transverse voltage $V_{xy}^{1\omega}$ is much smaller, it seems to appear due to the contacts mismatch. (b) Longitudinal $V_{xx}^{2\omega}$ and transverse $V_{xy}^{2\omega}$ voltage components in dependence on the ac current I_{ac} amplitude. $V_{xx}^{2\omega}$ is about zero, as it should be expected for the linear Ohmic $V_{xx}^{1\omega}$ (I_x^{ac}) curve. In contrast, there is significant transverse second-harmonic voltage $V_{xy}^{2\omega}$, which is non-linear and follows to $(I_{ac})^2$ law, as it is shown in the inset. This behavior well corresponds to thermoelectric origin of $V_{xy}^{2\omega} \sim \nabla T$.

consists of two $\sim 1/I_{dc}$ branches with sharp switching between them around zero bias, see Fig. 3 (a). Surprisingly, there is inversion of the thermoelectric response sign with the direction of I_{dc} : $V_{xy}^{2\omega}$ is negative for $I_{dc} < 0$, while it is positive for positive current values.

We wish to note, that the dc current contribution to Joule heating $\sim (I_{dc})^2$ is not sensitive to the current direction. Also, longitudinal dc bias I_{dc} can not be electrically detected in the transverse ac second-harmonic response $V_{xy}^{2\omega}$. On the other hand, the odd antisymmetric second-harmonic $V_{xy}^{2\omega}(I_{dc})$ curve is in sharp contrast to usual symmetric resistance behavior, which is shown as first-harmonic longitudinal $V_{xx}^{1\omega}$ in the upper inset to Fig. 3 (a). The first-harmonic transverse voltage $V_{xy}^{1\omega}$ is small, it qualitatively reproduces the $V_{xx}^{1\omega}$ behavior, as one could expect for small contact mismatch, see the lower inset to Fig. 3 (a).

We check, that $V_{xy}^{2\omega}$ still reflects the sample thermoelectric response at any finite I_{dc} . Fig. 3 (b) shows $V_{xy}^{2\omega} \sim (I_{ac})^2$ dependence for several fixed I_{dc} values, the curves differ only by proportionality coefficient, which depends on the sign and value of I_{dc} as $\sim 1/I_{dc}$. Thus, the direction of I_{dc} indeed affects the direction of the temperature gradient $\nabla T \sim V_{xy}^{2\omega}$, which can not be due to the dc current contribution to Joule heating $\sim (I_{dc})^2$.

The antisymmetric behavior of $V_{xy}^{2\omega}(I_{dc})$ is indepen-

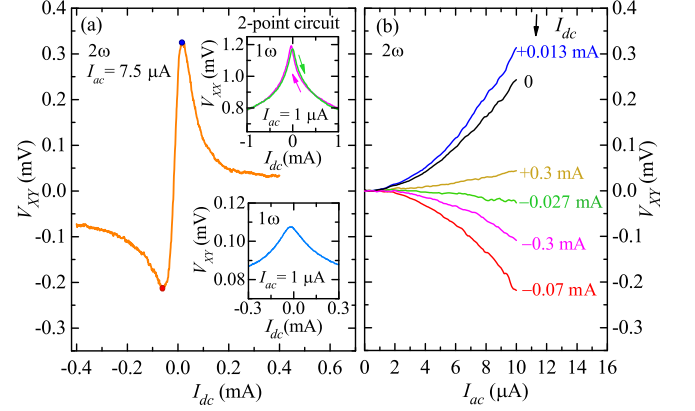


Figure 3. (Color online) (a) Dependence of the thermoelectric response $V_{xy}^{2\omega}$ on the dc bias current I_{dc} , which is applied between the same contacts C1 and C4 as the ac current component. The curve is strongly non-monotonous, it consists of two $\sim 1/I_{dc}$ branches with sharp switching between them around zero dc bias: $V_{xy}^{2\omega}$ is negative for $I_{dc} < 0$, while it is positive for positive current values. Upper inset demonstrates first-harmonic longitudinal $V_{xx}^{1\omega}$ component, which reflects sample differential resistance. Two curves are shown for two opposite sweep directions, which reflects ferroelectric hysteresis, see Ref. [28] for details. Lower inset shows first-harmonic transverse voltage $V_{xy}^{1\omega}$. It differs significantly from the second-harmonic one in the main plot, and strongly resembles the xx component due to the contacts mismatch. (b) Square-type thermoelectric dependence $V_{xy}^{2\omega} \sim (I_{ac})^2$ for several fixed I_{dc} values, $I_{dc} = +0.3; +0.013; 0; -0.027; -0.07; -0.3$ mA. The curves differ only by proportionality coefficient, which depends on the value and sign of I_{dc} as $\sim 1/I_{dc}$. This behavior well confirms thermoelectric origin of $V_{xy}^{2\omega} \sim \nabla T$ at any I_{dc} value, so it is the temperature gradient ∇T which depends as $\sim 1/I_{dc}$ law.

dent of the particular choice of contacts or any specific direction within SnSe flake. Fig. 4 (a) shows qualitatively similar $V_{yx}^{2\omega} \sim 1/I_{dc}$ dependence for the exchanged current and voltage probes in comparison to Fig. 1. In this case both current components I_{dc} and I_{ac} are applied in y direction between contacts C2 and C6, while transverse $V_{yx}^{2\omega}$ is measured along x between contacts C1 and C4, just opposite to the configuration in Fig. 1. Thus, the antisymmetric behavior of $V_{yx}^{2\omega}(I_{dc})$ is not connected with any specific sample inhomogeneity.

These results can be also qualitatively reproduced for the sample with much higher resistance (about 20 kOhm). Fig. 4 (b) shows antisymmetric odd $V_{xy}^{2\omega}(I_{dc})$ dependence, while the I_{dc} range is narrowed in this case. Due to the resistive sample, it is possible to directly apply bias voltage to the heating contacts in Fig. 1. The result is shown in the inset to Fig. 4 (b) as antisymmetric $V_{xy}^{2\omega}(V_{dc})$ curve with two $\sim 1/V_{dc}$ branches, so the sign of the thermoelectric response is determined by the direction

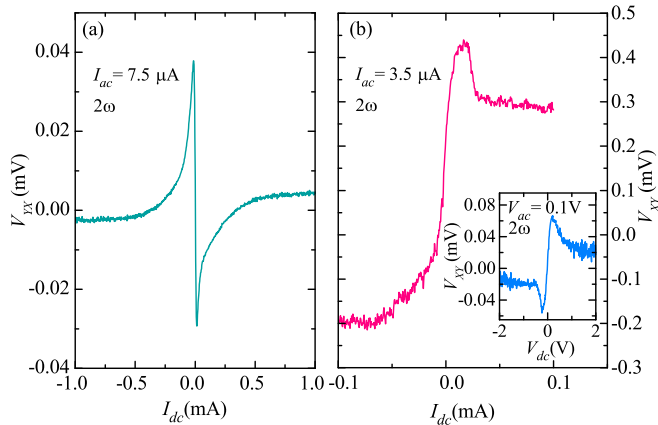


Figure 4. (a) Qualitatively similar $V_{yx}^{2\omega} \sim 1/I_{dc}$ dependence for the exchanged current and voltage probes in Fig. 1. Both current components I_{dc} and I_{ac} are applied along y between contacts C2 and C6, while $V_{yx}^{2\omega}$ is measured between contacts C1 and C4 (x axis). There are additional high-bias crossing points, however, ∇T sign inversion around zero bias is similar to the the previous configuration. Thus, antisymmetric behavior of $V_{xy}^{2\omega}(I_{dc})$ is not connected with any specific direction in the sample. (b) Similar results for the sample with much higher resistance (about 20 kOhm), while the I_{dc} range is narrowed in this case. Inset shows $V_{xy}^{2\omega}(V_{dc})$ curve with two $\sim 1/V_{dc}$ branches if the bias voltage is directly applied to the heating contacts in Fig. 1. Thus, the sign of the thermoelectric response is indeed determined by the direction of the in-plane dc electric field.

of the in-plane dc electric field.

DISCUSSION

As a result, we demonstrate that the transverse second-harmonic ac voltage response $V_{xy}^{2\omega}$ indeed reflects temperature gradient ∇T at any I_{dc} value. To our surprise, ∇T obeys $\sim 1/I_{dc}$ dependence with inversion of the ∇T sign with the direction of I_{dc} .

First of all, ∇T sign inversion can not be explained by simple geometrical factor. In Fig. 1 temperature gradient ∇T is measured between 80 μm spaced contacts C2 and C6, while the distance between heating contacts C1 and C4 is about 40 μm . Since the contact resistance exceeds the bulk SnSe value [23], Joule heating is mostly concentrated in the contact areas. Since two-point resistance strongly depends on the dc bias in the upper inset to Fig. 3 (a), the bias changes relative contribution of the particular contact to the Joule heating. It leads to some variation of ∇T direction between C6-C1 and C6-C4 lines in Fig. 1, i.e. within $\approx \pm 15$ degrees, so it can not change ∇T sign in Fig. 3 and in Fig. 4 (b). In contrast, the curve in Fig. 4 (a) is obtained in the alternative ge-

ometry, where voltage probes are situated to both sides from the current line. In this case, ∇T sign inversion is possible at high dc biases, which seems to be responsible for the additional high-bias crossing points in Fig. 4 (a). However, $\nabla T \sim 1/I_{dc}$ dependence around zero bias does not allow geometrical explanation also in this case.

The first power of I_{dc} indicates that ∇T is sensitive to the sign and value of the dc electric field. However, it can not be connected with the Peltier effect, since ∇T is proportional to $\sim 1/I_{dc}$ rather than the expected $\sim I_{dc}$ dependence for the Peltier effect.

On the other hand, electrocaloric effect should principally be observable in ferroelectric conductors. In contrast to standard ferroelectric insulator films [12, 14, 15], it can be produced by in-plane current-induced electric field in conducting ferroelectric systems.

Recently, three-dimensional WTe₂ single crystals were found to demonstrate coexistence of metallic conductivity and ferroelectricity at room temperature [4] due to the strong anisotropy of the non-centrosymmetric crystal structure. The spontaneous polarization of ferroelectric domains was found to be bistable, it can be affected by high external electric field. The possibility to induce polarization current by source-drain field variation has been shown for WTe₂ as a direct consequence of ferroelectricity and metallic conductivity coexistence [28]. We have demonstrated qualitatively similar ferroelectric behavior of $dV/dI(I)$ curves for thin SnSe flakes [23], as it is shortly shown in the present text as small hysteresis for $V_{xx}^{1\omega}(I)$ in the upper inset to Fig. 3.

Thin SnSe layers (300 nm and below) are characterized [22] by in-plane spontaneous ferroelectric polarization at room temperature. Ferroelectric domains are much smaller than the contact size in our samples [22]: the domains are about 100 nm, the domain wall region is about 20-50 nm. In this case, any variation of the source-drain bias I_{dc} affects ferroelectric polarization due to the domain wall shift for varying $E \sim I_{dc}$ in-plane electric field [23]. It leads to the temperature variation because of the electrocaloric effect [13, 14, 29], so the sign of the temperature δT variation δT is determined by the direction of the electric field E .

More precisely, E/T ratio is a constant in the conditions of electrocaloric effect. Thus, $\delta(E/T)$ is zero, which gives $\delta T = (T/E)\delta E$. In our experiment, we measure only $T\delta E$ component which is proportional to $(I_{ac})^2$ due to the 2ω lock-in detection technique, while the in-plane electric field $E \sim I_{dc} \sim V_{dc}$. It gives exactly $\nabla T \sim (I_{ac})^2/I_{dc}$ dependence, which we observe in Figs. 3 and 4.

From the $V_{xy}^{2\omega}$ values within ± 0.3 mV one can estimate [21] maximum temperature variation as $\Delta T \approx \pm 0.5$ K. This value well corresponds for the known one (mostly 2-5 K) in insulating ferroelectric crystals [8] or thin films [12, 14, 15]. Thus, we not only demonstrate possibility to create electrocaloric effect by current-

induced electric field in conducting ferroelectric crystals, but also obtain competitive values of the effect.

CONCLUSION

As a conclusion, we experimentally investigate thermoelectric response of a 100 nm thick SnSe single crystal flake under the current-induced dc electric field. Thermoelectric response appears as a second-harmonic transverse voltage $V_{xy}^{2\omega}$, which reflects temperature gradient across the sample due to the Joule heating by harmonic ac excitation current I_{ac} . In addition to strongly non-monotonous dependence $V_{xy}^{2\omega}$, we observe that dc field direction controls the sign of the temperature gradient in the SnSe flake. We provide arguments, that electrocaloric effect is the mostly probable reason for the results obtained. Thus, our experiment can be understood as demonstration of the possibility to induce electrocaloric effect by in-plane electric field in conducting ferroelectric crystals and to detect it by thermoelectric response.

ACKNOWLEDGEMENT

We wish to thank V.T. Dolgoplov for fruitful discussions, and S.S Khasanov for X-ray sample characterization. We gratefully acknowledge financial support partially by the RFBR (project No. 19-02-00203), and RF State task.

-
- [1] As a recent review see N.P. Armitage, E.J. Mele, and A. Vishwanath, *Rev. Mod. Phys.* 90, 015001 (2018).
- [2] A. Manchon, J. Zelezný, I. M. Miron, T. Jungwirth, J. Sinova, A. Thiaville, K. Garello, and P. Gambardella, *Reviews of Modern Physics* 91, 035004 (2019).
- [3] Salvador Barraza-Lopez, Benjamin M. Fregoso, John W. Villanova, Stuart S. P. Parkin, Kai Chang, *Rev. Mod. Phys.*, Vol. 93, No. 1, 011001-3 (2021).
- [4] P. Sharma, F.-X. Xiang, D.-F. Shao, D. Zhang, E.Y. Tsymlal, A.R. Hamilton, and J. Seide, *Sci. Adv.* 5(7), eaax5080 (2019).
- [5] Kenji Yasuda, Xirui Wang, Kenji Watanabe, Takashi Taniguchi, Pablo Jarillo-Herrero, *Science*, eabd3230 (2021) DOI: 10.1126/science.abd3230. arXiv:2010.06600
- [6] V. V. Enaldiev, F. Ferreira, S. J. Magorrian, Vladimir I. Fal'ko, *2D Mater.* 8 025030 (2021) (2021).
- [7] B. Li, X. Zhang, J.B. Wang, X.L. Zhong, F. Wang, Y.C. Zhou, *Mechanics Research Communications* 55, 40 (2014).
- [8] S. Merselmiz, Z. Hanani, D. Mezzane, M. Spreitzer, A. Bradeško, D. Fabijan, D. Vengust, M'Barek Amjoud, L. Hajji, Z. Abkhar, et al., *Ceramics International* 46, 23867 (2020).
- [9] Matjaz Valant, *Progress in Materials Science* 57, 980 (2012).
- [10] Junye Shi, Donglin Han, Zichao Li, Lu Yang, Sheng-Guo Lu, Zhifeng Zhong, Jiangping Chen, Q.M. Zhang, Xiaoshi Qian, *Joule* 3, 1200 (2019).
- [11] I. Ponomareva and S. Lisenkov, *Phys. Rev. Lett.* 108, 167604 (2012).
- [12] B. Nair, T. Usui, S. Crossley, S. Kurdi, G. G. Guzmán-Verri, X. Moya, S. Hirose, N. D. Mathur, *Nature* 575, 468 (2019).
- [13] S. Lisenkov and I. Ponomareva, *Phys. Rev. B* 80, 140102(R) (2009).
- [14] Hao Chen, Tian-Ling Ren, Xiao-Ming Wu, Yi Yang, and Li-Tian Liu, *Appl. Phys. Lett.* 94, 182902 (2009).
- [15] Qiu, J.H., Jiang, Q., *J. Appl. Phys.* 103, 34119, 1 (2008).
- [16] K. Co, H. Khassaf, and S. P. Alpay, *J. Appl. Phys.* 127, 174102 (2020).
- [17] J.Železný, Z. Fang, K. Olejník, J. Patchett, F. Gerhard, C. Gould, L. W. Molenkamp, C. Gomez-Olivella, J. Zemen, T. Tichý, T. Jungwirth, C. Ciccarelli, arXiv:2102.12838.
- [18] O. O. Shvetsov, V. D. Esin, A. V. Timonina, N. N. Kolesnikov, and E. V. Deviatov, *JETP Letters*, 109, 715 (2019).
- [19] V. D. Esin, A. V. Timonina, N. N. Kolesnikov, E. V. Deviatov, *JETP Letters*, 111, pp. 685 (2020)
- [20] A. Mokashi, S. Li, B. Wen, S. V. Kravchenko, A. A. Shashkin, V. T. Dolgoplov, and M. P. Sarachik, *Phys. Rev. Lett.* 109, 096405 (2012).
- [21] L.-D. Zhao, Sh.-H. Lo, Y. Zhang, H. Sun, G. Tan, C. Uher, C. Wolverton, V. P. Dravid and M. G. Kanatzidis, *Nature* 508, 373 (2014).
- [22] K. Chang, F. Küster, B. J. Miller, J.-R. Ji, J.-L. Zhang, P. Sessi, S. Barraza-Lopez, and S. S. P. Parkin, *Nano Lett.* 20(9), 6590 (2020).
- [23] N.N. Orlova, A.V. Timonina, N.N. Kolesnikov, E.V. Deviatov, arXiv:2012.06385 (2020).
- [24] Shengxue Yang, Yuan Liu, Minghui Wu, Li-Dong Zhao, Zhaoyang Lin, Hung-chieh Cheng, Yiliu Wang, Chengbao Jiang, Su-Huai Wei, Li Huang, Yu Huang, and Xiangfeng Duan, *Nano Res.* 11(1), 554 (2018).
- [25] O.O. Shvetsov, V.D. Esin, A.V. Timonina, N.N. Kolesnikov, and E.V. Deviatov, *Phys. Rev. B* 99, 125305 (2019).
- [26] V.D. Esin, D.N. Borisenko, A.V. Timonina, N.N. Kolesnikov, and E.V. Deviatov, *Phys. Rev. B* 101, 155309 (2020).
- [27] N.N. Orlova, N.S. Ryshkov, A.A. Zagitova, V.I. Kulakov, A.V. Timonina, D.N. Borisenko, N.N. Kolesnikov, and E.V. Deviatov, *Phys. Rev. B* 101, 235316 (2020)
- [28] N.N. Orlova, N.S. Ryshkov, A.V. Timonina, N.N. Kolesnikov, and E.V. Deviatov, *Jetp Lett.* 113, 389 (2021) <https://doi.org/10.1134/S0021364021060011>
- [29] Gang Bai, Xueshi Qin, Qiyun Xie, Cunfa Gao, *Physica B: Condensed Matter* 560, 208 (2019).